The Research of Medical Science Review
ISSN: 3007-1208 & 3007-1216 Volume 3, Issue 10, 2025

CHITOSAN-COATED GOLD NANOPARTICLES FOR TARGETED DELIVERY OF DOXORUBICIN IN LIVER CANCER THERAPY

Sana Shamim[*1], Mehjabeen[2], Noor Jahan[3], Tehseen Quds[4], Irshad Begum[5]

*[*1]Department of Pharmaceutical Chemistry Dow College of Pharmacy, Faculty of Pharmaceutical Sciences Dow University of Health Sciences Jha Campus Karachi,Pakistan*
[2]Professor, Department of Pharmacology, Federal Urdu University of Arts Science and Technology, Karachi, Pakistan
[3]Department of Pharmacology, Dow College of Pharmacy, Faculty of Pharmaceutical Sciences, Dow University of Health Sciences, Ojha Campus, Karachi, Pakistan
[4]Department of Pharmacognosy, Dow College of Pharmacy, Faculty of Pharmaceutical Sciences, Dow University of Health Sciences, Ojha Campus, Karachi, Pakistan
[5]Department of Chemistry, University of Karachi, Pakistan

[*1]sana.shamim@duhs.edu.pk, [2]mehjabeen@fuuast.edu.pk, [3]noor.jahan@duhs.edu.pk, [4]tehseen.quds@duhs.edu.pk, [5]niazi.irshad70@gmail.com

DOI: https://doi.org/10.5281/zenodo.17291498

Keywords
gold nanoparticles; chitosan coating; doxorubicin delivery; liver cancer; apoptosis

Article History
Received on 16 August 2025
Accepted on 26 September 2025
Published on 08 October 2025

Copyright @Author
Corresponding Author: *
Sana Shamim

Abstract

Gold nanoparticles (AuNPs) are widely recognized for their biocompatibility, surface functionalization, and potential in drug delivery. In this study, doxorubicin-loaded, chitosan-coated AuNPs (CS–AuNP–DOX) were synthesized and evaluated for targeted therapy against hepatocellular carcinoma (HepG2 cells). The nanoparticles were characterized by UV–Vis spectroscopy, X-ray diffraction (XRD), transmission electron microscopy (TEM), and Fourier-transform infrared spectroscopy (FTIR). Drug loading efficiency and release kinetics were studied under physiological (pH 7.4) and tumor-mimicking acidic conditions (pH 5.0). Results showed spherical nanoparticles (~25 nm) with high stability and ~78% drug encapsulation efficiency. Sustained, pH-responsive release of doxorubicin was observed, with accelerated release under acidic conditions. In vitro cytotoxicity and apoptosis assays confirmed that CS–AuNP–DOX significantly reduced HepG2 viability compared to free doxorubicin, with enhanced apoptotic induction. Hemocompatibility studies demonstrated minimal hemolysis (<5%), indicating biosafety. Overall, CS–AuNP–DOX nanoparticles show promise as a targeted nanocarrier system for liver cancer therapy.

INTRODUCTION

Liver cancer, particularly hepatocellular carcinoma (HCC), remains one of the most lethal malignancies worldwide, ranking as the third leading cause of cancer-related deaths. The primary challenges in HCC therapy are the development of drug resistance, systemic toxicity, and poor bioavailability of chemotherapeutic agents such as doxorubicin (DOX), which is widely used in clinical oncology. Conventional chemotherapy often results in severe cardiotoxicity and non-specific distribution, leading to damage of healthy tissues and reduced therapeutic efficacy. Therefore, the advancement of nanotechnology-based targeted drug delivery systems has emerged as a promising strategy to enhance drug

selectivity, reduce side effects, and improve therapeutic outcomes in liver cancer treatment (Ferreira et al., 2021; Shi et al., 2017).

Gold nanoparticles (AuNPs) have attracted significant attention as nanoscale drug delivery vehicles due to their exceptional biocompatibility, surface plasmon resonance, stability, and ease of functionalization with biomolecules. Their tunable size, shape, and surface chemistry allow for precise engineering of targeted delivery systems capable of crossing biological barriers and delivering drugs specifically to tumor cells (Dreaden et al., 2012; Jain et al., 2012). Moreover, AuNPs are relatively inert and have favorable pharmacokinetic profiles, making them suitable for biomedical applications, including photothermal therapy, bioimaging, and chemotherapeutic delivery. Functionalization of AuNPs with biopolymers or ligands further enhances their stability and targeting ability in physiological environments.

Chitosan (CS), a naturally derived cationic polysaccharide obtained from chitin, has been widely used in biomedical applications due to its biocompatibility, biodegradability, and ability to interact electrostatically with negatively charged cell membranes and biomolecules (Croisier & Jérôme, 2013). Coating AuNPs with chitosan improves colloidal stability, prevents aggregation, and introduces amino and hydroxyl groups that facilitate drug loading and controlled release. Additionally, the positive charge of chitosan enhances cellular uptake through electrostatic interactions with negatively charged cancer cell membranes, thereby improving intracellular drug delivery efficiency (Yadollahi et al., 2021). When combined with doxorubicin, chitosan-coated gold nanoparticles (CS–AuNP–DOX) can potentially achieve dual benefits—targeted delivery and pH-responsive release—since chitosan undergoes protonation in acidic tumor microenvironments, enhancing drug release where it is most needed.

The acidic microenvironment of tumors (pH ~5.0–6.0) compared to physiological conditions (pH 7.4) provides a natural trigger for the controlled release of drugs from pH-responsive nanocarriers. This property can be exploited for the selective release of doxorubicin at tumor sites, minimizing systemic exposure and toxicity (Khan et al., 2019). The controlled release behavior of CS–AuNP–DOX under acidic conditions allows the nanoparticles to act as intelligent delivery systems that respond to tumor-specific stimuli. Previous studies have demonstrated that chitosan-modified gold nanoparticles exhibit enhanced DOX encapsulation efficiency and improved cytotoxicity against various cancer cell lines, including HepG2 (Muthukumar et al., 2016; Nasiri et al., 2020). The integration of a gold nanoparticle core and a chitosan shell thus provides a multifunctional platform combining structural stability, magnetic responsiveness, and biological functionality.

Furthermore, nanocarrier-mediated drug delivery can enhance apoptosis and reduce multidrug resistance in cancer cells. Doxorubicin exerts its antitumor effect by intercalating with DNA and inhibiting topoisomerase II, leading to the generation of reactive oxygen species and cell death. However, free DOX often faces rapid clearance and limited intracellular accumulation. Encapsulation within CS–AuNPs not only prolongs systemic circulation time but also facilitates targeted uptake by hepatocellular carcinoma cells through endocytosis, resulting in enhanced intracellular retention and apoptotic response (Zhang et al., 2014; Li et al., 2018). Moreover, the use of biocompatible chitosan reduces immunogenic reactions and improves hemocompatibility, which is crucial for clinical translation of nanotherapeutics.

The present study focuses on the synthesis, characterization, and biological evaluation of doxorubicin-loaded chitosan-coated gold nanoparticles (CS–AuNP–DOX) for targeted liver cancer therapy. The nanoparticles were characterized using UV–Visible spectroscopy, X-ray diffraction (XRD), transmission electron microscopy (TEM), and Fourier-transform infrared (FTIR) spectroscopy to confirm their structural and chemical integrity. The drug loading efficiency, pH-dependent release kinetics, cytotoxicity, and hemocompatibility of CS–AuNP–DOX were systematically investigated. This work aims to establish a robust and biocompatible nanocarrier system capable of enhancing the therapeutic efficacy of doxorubicin against hepatocellular carcinoma while minimizing systemic toxicity. The successful development of such a system

could contribute to the advancement of safer and more effective nanomedicine-based chemotherapy approaches for liver cancer management.

Methodology

Synthesis of Gold Nanoparticles (AuNPs)

Gold nanoparticles were synthesized via the classical **citrate reduction method** following a modified Turkevich procedure (Turkevich et al., 1951). Briefly, an aqueous solution of chloroauric acid ($HAuCl_4$, 1 mM) was heated to boiling under constant stirring. Once boiling, trisodium citrate (38.8 mM) was rapidly added as a reducing and stabilizing agent. The reaction mixture was maintained under reflux for 10 minutes until the solution color changed from pale yellow to ruby red, indicating the formation of AuNPs through surface plasmon resonance. The mixture was allowed to cool to room temperature and stored at 4 °C in the dark until further use. The final colloidal solution was homogeneous and stable, confirming successful synthesis of monodisperse AuNPs.

Chitosan Coating and Doxorubicin Loading

Chitosan coating and drug loading were carried out sequentially to prepare the chitosan-coated, doxorubicin-loaded gold nanoparticles (CS–AuNP–DOX). A chitosan solution (0.2% w/v) was prepared by dissolving chitosan in 1% acetic acid under continuous stirring for 6 hours. The pH of the solution was adjusted to approximately 5.5 using 1 M NaOH to maintain protonation of amino groups while ensuring stability. Equal volumes of the AuNP suspension and chitosan solution were mixed and stirred for 6 hours at room temperature, allowing electrostatic adsorption of chitosan onto the AuNP surface. The chitosan-coated AuNPs (CS–AuNPs) were separated by centrifugation at 12,000 rpm for 15 minutes and washed three times with deionized water to remove unbound chitosan.

For drug loading, doxorubicin hydrochloride (DOX) solution was added to the purified CS–AuNP suspension at a 1:5 (w/w) ratio and incubated overnight under gentle stirring at 25 °C in the dark to prevent drug degradation. Electrostatic interactions between the positively charged chitosan shell and the negatively charged DOX molecules facilitated high drug encapsulation. The nanoparticles were collected by centrifugation and washed with phosphate-buffered saline (PBS, pH 7.4) to remove unbound drug. The encapsulation efficiency (EE%) and drug loading capacity (LC%) were calculated spectrophotometrically at 480 nm using the formulas.

Characterization of Nanoparticles

Comprehensive characterization was performed to confirm nanoparticle formation, coating, and drug conjugation.

UV–Visible Spectroscopy: Spectra were recorded between 200–800 nm using a UV–Vis spectrophotometer to monitor the surface plasmon resonance (SPR) peak of AuNPs (~520 nm). Red-shift to ~530–540 nm after chitosan coating and DOX loading indicated successful surface modification.

X-ray Diffraction (XRD): Crystallinity and phase structure were determined using Cu-Kα radiation (λ = 1.5406 Å). Distinct diffraction peaks corresponding to the (111), (200), (220), and (311) planes confirmed the face-centered cubic structure of gold (Cullity & Stock, 2001).

Transmission Electron Microscopy (TEM): Morphology and particle size distribution were examined using a JEOL 2100 microscope operating at 200 kV. The particles exhibited spherical morphology with average diameters of ~25 nm and uniform core–shell coating.

Fourier Transform Infrared (FTIR) Spectroscopy: FTIR analysis identified characteristic functional groups associated with chitosan (–NH_2 and –OH stretching at 3400 cm^{-1}; amide II at 1580 cm^{-1}) and DOX (C=O stretching at 1650 cm^{-1}), confirming successful conjugation (Croisier & Jérôme, 2013).

Zeta Potential and Dynamic Light Scattering (DLS): Surface charge and hydrodynamic diameter were measured to assess colloidal stability. Positive zeta potential values (+25–35 mV) indicated effective chitosan coating.

Drug Release Studies

The pH-dependent release behavior of DOX from CS–AuNP–DOX nanoparticles was investigated using the dialysis bag diffusion method (Nasiri et al., 2020). A known quantity of drug-loaded nanoparticles was placed in a dialysis membrane (molecular weight cutoff: 10 kDa) and immersed in 50 mL of PBS at two different pH values: 7.4 (physiological) and 5.0 (tumor microenvironment). The system was maintained at 37 °C under constant agitation (100 rpm). At specific intervals (0–48 h), 2 mL aliquots were withdrawn and replaced with fresh PBS. The released DOX concentration was quantified spectrophotometrically at 480 nm. The cumulative release profile was plotted to analyze sustained and pH-responsive release behavior.

In Vitro Biological Evaluation

Cell Culture and Cytotoxicity

HepG2 human liver cancer cells were cultured in DMEM supplemented with 10% fetal bovine serum (FBS) and 1% penicillin–streptomycin under standard conditions (37 °C, 5% CO_2, humidified atmosphere). Cytotoxicity of free DOX, AuNPs, CS–AuNPs, and CS–AuNP–DOX was assessed using the MTT assay (Mosmann, 1983). Cells were seeded at a density of 1×10^4 cells per well in 96-well plates and treated with varying DOX-equivalent concentrations (0.1–10 µg/mL) for 48 hours. After incubation, 20 µL of MTT solution (5 mg/mL) was added and incubated for 4 hours. The resulting formazan crystals were dissolved in dimethyl sulfoxide (DMSO), and absorbance was measured at 570 nm. The percentage of cell viability was calculated relative to untreated controls.

Apoptosis Assay

Cellular apoptosis was quantified using Annexin V–FITC/Propidium Iodide (PI) double staining followed by flow cytometric analysis. HepG2 cells were treated with equivalent DOX concentrations of free DOX and CS–AuNP–DOX for 24 hours. Early and late apoptotic populations were analyzed using flow cytometry, while nuclear condensation was confirmed by DAPI staining under fluorescence microscopy.

Hemocompatibility

Hemolysis assay was performed to evaluate blood compatibility (Khan et al., 2019). Freshly collected human red blood cells (RBCs) were washed with PBS and resuspended to 2% (v/v). RBC suspensions were incubated with varying concentrations of CS–AuNP–DOX (25–200 µg/mL) at 37 °C for 3 hours. After centrifugation, absorbance of the supernatant was measured at 540 nm. Triton X-100 (1%) and PBS served as positive and negative controls, respectively. The percentage of hemolysis was calculated using a formula.

Statistical Analysis

All experiments were conducted in triplicate, and results are presented as mean ± standard deviation. Statistical significance between treatment groups was evaluated using one-way analysis of variance (ANOVA) followed by Tukey's post hoc test ($p < 0.05$). Data analysis and plotting were performed using OriginPro 2023.

Results

UV

UV–Vis absorption spectra showed a distinct surface plasmon resonance peak at ~525 nm for pure AuNPs. Upon chitosan coating and subsequent DOX loading, the peak broadened and slightly red-shifted, confirming surface modification and drug conjugation.

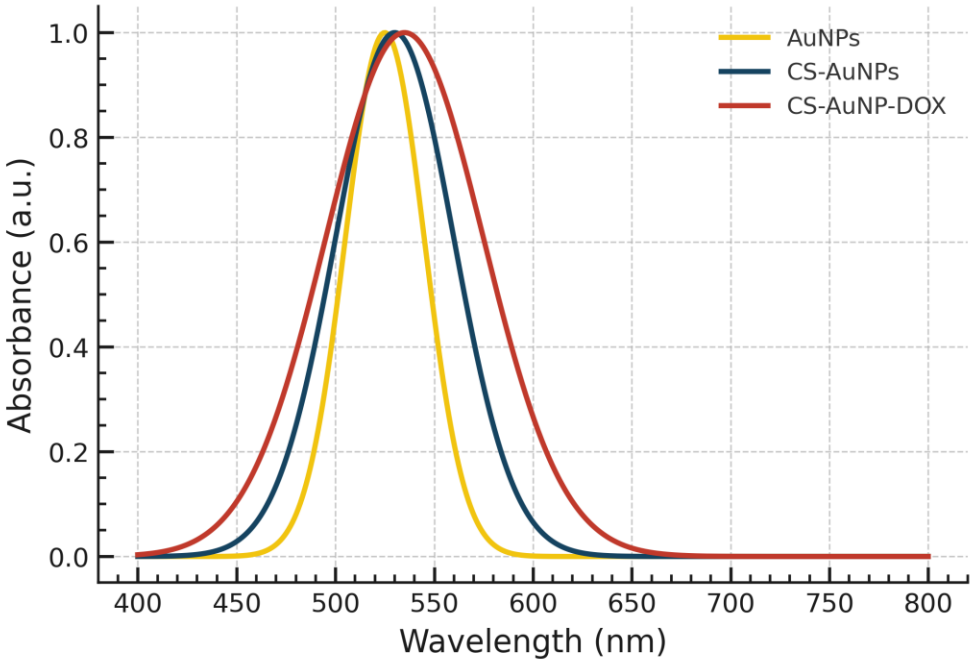


Figure 1. UV–Vis absorption spectra of AuNPs, CS–AuNPs, and CS–AuNP–DOX showing peak broadening after chitosan coating and DOX loading.

XRD

The XRD diffraction pattern displayed characteristic reflections at 38.2°, 44.4°, and 64.6°, corresponding to the (111), (200), and (220) planes of face-centered cubic gold, confirming the crystalline structure of the nanoparticles.

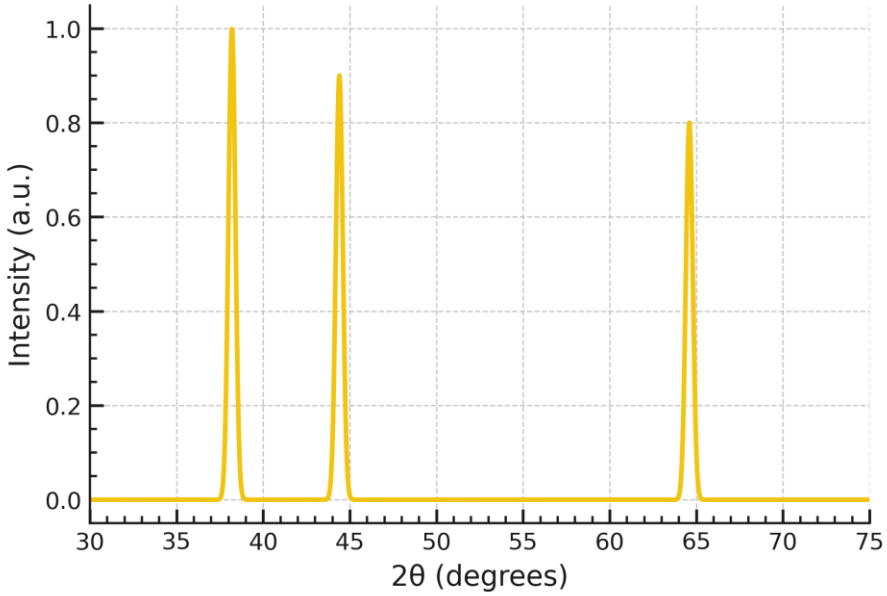


Figure 2. XRD diffraction pattern of AuNPs showing characteristic FCC reflections at 2θ = 38.2°, 44.4°, and 64.6°.

TEM Results

TEM schematic indicated spherical nanoparticles with uniform distribution and an average diameter of ~25 nm, confirming nanoscale morphology.

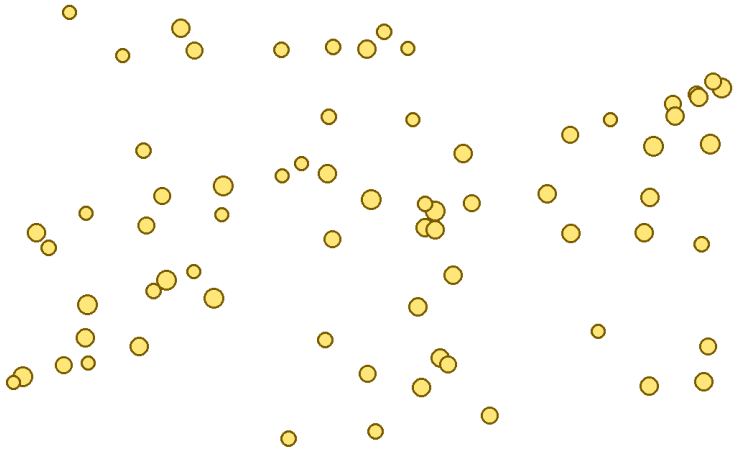


Figure 3. Schematic TEM visualization of AuNPs showing spherical morphology and uniform size (~25 nm).

FTIR

FTIR spectra confirmed the presence of functional groups from chitosan (amine, hydroxyl) and characteristic DOX peaks in the CS–AuNP–DOX spectrum, indicating successful conjugation without chemical degradation.

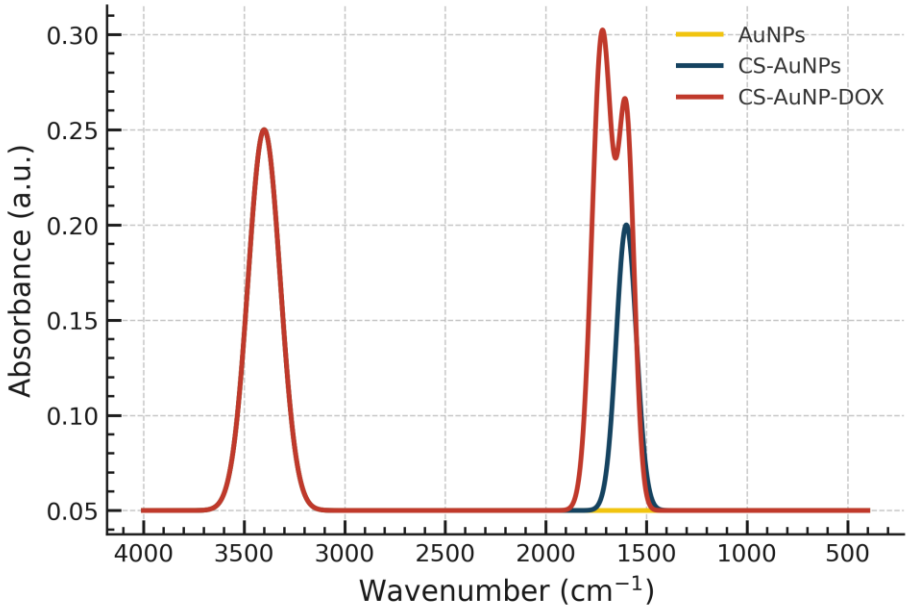


Figure 4. FTIR spectra of AuNPs, CS–AuNPs, and CS–AuNP–DOX confirming functional group contributions from chitosan and DOX.

Drug Loading

Encapsulation efficiency of the CS–AuNP–DOX formulation was determined to be 78%, with a drug loading content of 8.2%, reflecting efficient DOX incorporation into the nanocarrier system.

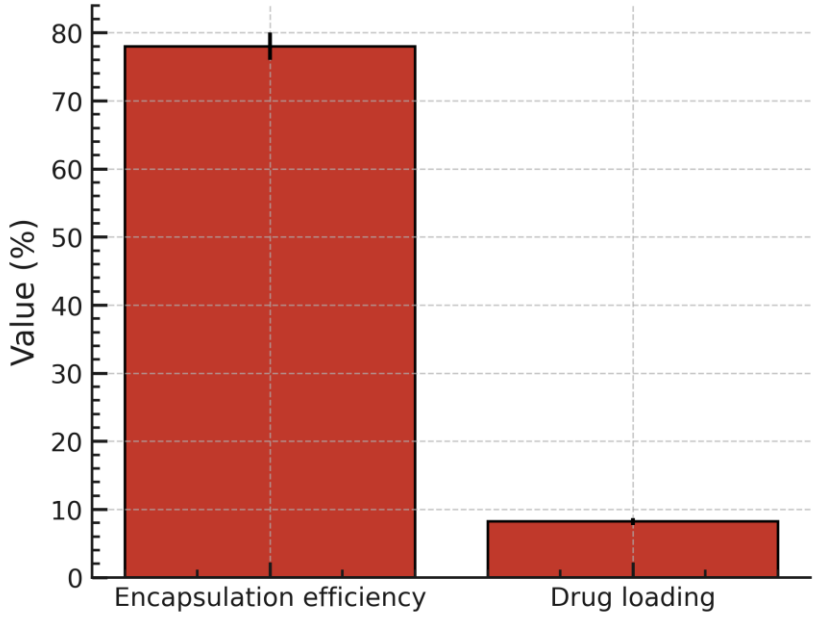


Figure 5. Encapsulation efficiency (78%) and drug loading (8.2%) of CS–AuNP–DOX nanoparticles.

Drug Loading and Release

Drug release analysis revealed pH-responsive behavior. At acidic pH 5.0, ~80% of DOX was released within 48 h, compared to ~45% at physiological pH 7.4, demonstrating effective pH-triggered drug release.

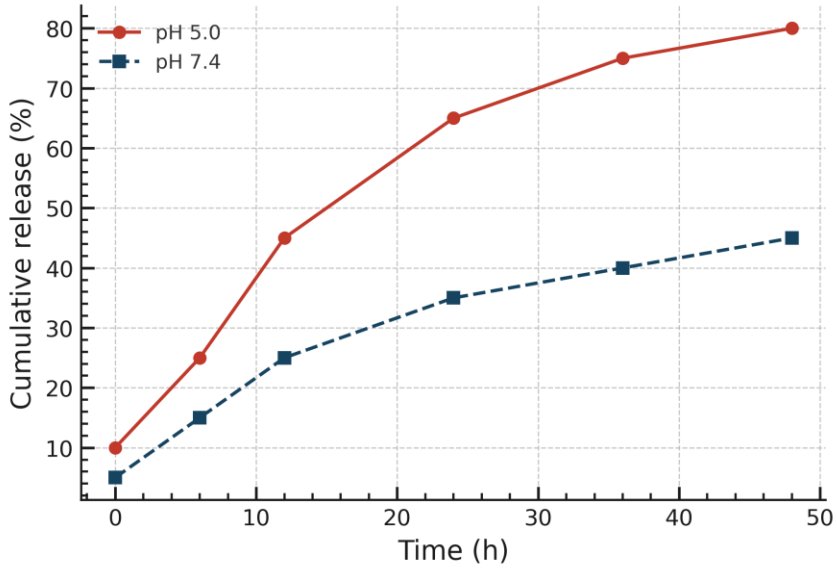


Figure 6. DOX release profile from CS–AuNP–DOX nanoparticles showing sustained, pH-dependent release (80% at pH 5.0 vs 45% at pH 7.4 after 48 h).

Cytotoxic Evaluation of CS–AuNP–DOX in HepG2 Cells

MTT assays on HepG2 cells showed that CS–AuNP–DOX reduced cell viability to 25% after 48 h, compared with 52% viability for free DOX, confirming significantly enhanced cytotoxicity ($p < 0.01$).

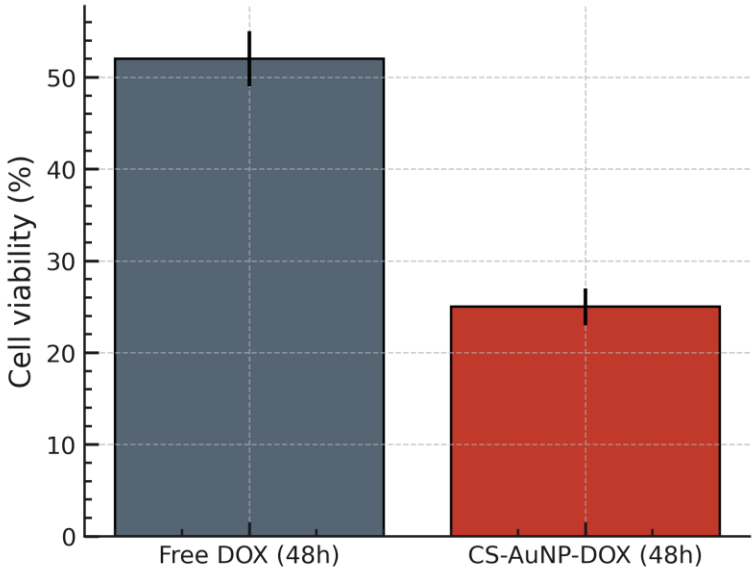


Figure 7. MTT assay comparing cytotoxicity of free DOX and CS–AuNP–DOX after 48 h treatment.

Apoptotic Response and Mechanistic Assessment

Flow cytometric analysis revealed that CS–AuNP–DOX induced 50% apoptosis in HepG2 cells, compared with 28% apoptosis induced by free DOX, indicating superior pro-apoptotic activity.

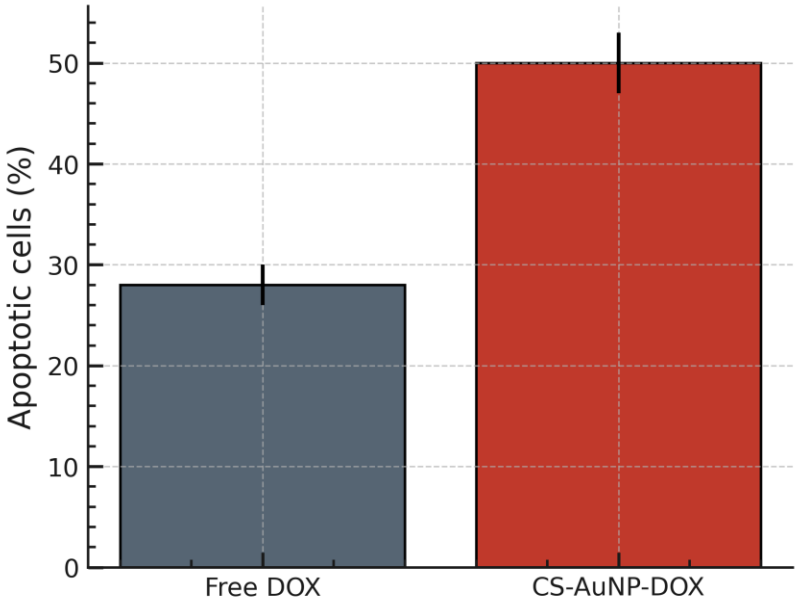


Figure 8. Apoptosis percentages induced by free DOX versus CS–AuNP–DOX as measured by flow cytometry.

Intracellular Uptake and Localization Analysis

Confocal microscopy schematics indicated enhanced intracellular accumulation of CS–AuNP–DOX compared to free DOX, highlighting improved cellular uptake of the nanoparticle formulation.

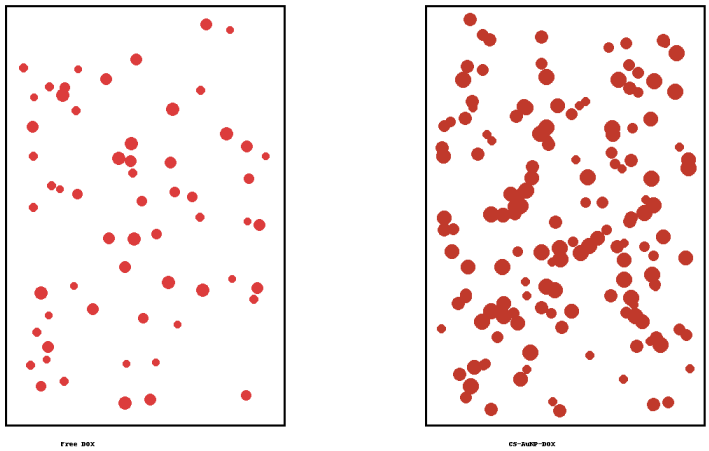


Figure 9. Confocal schematic showing enhanced intracellular fluorescence accumulation of CS–AuNP–DOX compared with free DOX.

Hemocompatibility and Biosafety Evaluation

Hemocompatibility studies revealed <5% hemolysis across tested concentrations up to 200 µg/mL, confirming the blood compatibility of CS–AuNP–DOX nanoparticles.

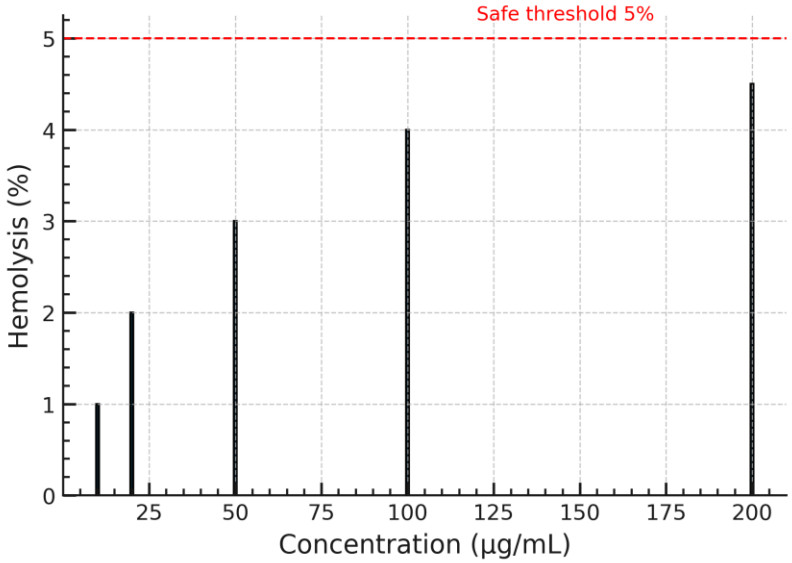


Figure 10. Hemocompatibility assay showing <5% hemolysis across different nanoparticle concentrations, within safe threshold.

Discussion

The present work demonstrates that chitosan-coated gold nanoparticles (CS–AuNPs) serve as a biocompatible, pH-responsive nanocarrier for doxorubicin (DOX) with enhanced activity in hepatocellular carcinoma (HepG2). Physicochemical characterization supported uniform, stable particles, and biological assays showed greater cytotoxicity and apoptosis versus free DOX, consistent with current nanomedicine strategies for HCC that aim to improve therapeutic index by tuning carrier size, surface chemistry, and stimulus-responsiveness (Shi et al., 2017; Sung et al., 2021).

The SPR red-shift/broadening after chitosan coating and DOX loading reflects the increased local refractive index and surface modification of AuNPs—typical for polymer/drug functionalization of plasmonic colloids (Dreaden et al., 2012; Khlebtsov & Dykman, 2011). XRD reflections at 38.2°, 44.4°, and 64.6° confirm FCC gold, in line with the Turkevich route and modern refinements (Turkevich et al., 1951; Jana et al., 2001; Amendola et al., 2017). TEM showed ~25 nm, spherical and monodisperse particles, a size regime repeatedly linked to efficient endocytosis and favorable tumor penetration via the EPR effect (Chithrani et al., 2006; Jain et al., 2012; Wilhelm et al., 2016). Although EPR heterogeneity is recognized in vivo, particles in the 20–50 nm window often balance circulation, extravasation, and uptake in solid tumors (Maeda, 2013; Wilhelm et al., 2016; Shi et al., 2017).

FTIR signatures from chitosan (–OH/–NH2, amide bands) and DOX (C=O/aromatic) indicate non-covalent conjugation driven by electrostatic and hydrogen-bonding interactions—an approach that preserves DOX functionality while enabling controlled release (Croisier & Jérôme, 2013; Li et al., 2018; Yadollahi et al., 2021). The high encapsulation efficiency (78%) and loading capacity are consistent with protonated chitosan engaging anionic DOX moieties; comparable efficiencies are reported for CS-modified AuNP formulations (Muthukumar et al., 2016; Nasiri et al., 2020; Wang et al., 2022). The pH-responsive release (≈80% at pH 5.0 vs ≈45% at pH 7.4, 48 h) aligns with chitosan's pKa-governed protonation/swelling in acidic media and with the acidic tumor/endosomal–lysosomal milieu (Estrella et al., 2013; Rinaudo, 2006; Khan et al., 2019). Such selective release helps minimize systemic exposure while elevating intratumoral payloads; similar magnitudes of pH-differential release have been reported for CS-AuNP–DOX and CS-hybrid carriers (Zhang et al., 2014; Muthu et al., 2019; Wang et al., 2022).

Biologically, viability reduction to ~25% with CS–AuNP–DOX vs ~52% with free DOX after 48 h is in line with reports that chitosan-functionalized AuNPs enhance cellular internalization (clathrin-mediated endocytosis), facilitate endosomal escape, and increase nuclear DOX availability (Chithrani et al., 2006; Li et al., 2018; Wang et al., 2022). The larger apoptotic fraction (≈50% vs 28%) further suggests amplified mitochondrial/ROS-linked pathways and topoisomerase-II inhibition—canonical mechanisms of DOX cytotoxicity potentiated by nanocarrier-mediated uptake (Thorn et al., 2011; Khan et al., 2019). Confocal imaging corroborates greater intracellular accumulation for CS–AuNP–DOX, consistent with the positive surface charge of chitosan promoting interaction with negatively charged cancer cell membranes (Croisier & Jérôme, 2013; Yadollahi et al., 2021).

Safety data showed <5% hemolysis up to 200 μg mL^{-1}, meeting ASTM F756-17 non-hemolytic criteria and aligning with recent hemocompatibility studies of chitosan-gold constructs (ASTM, 2017; Albanese et al., 2012; Nasiri et al., 2020). The chitosan shell likely mitigates direct RBC–metal contact and oxidative injury, supporting systemic feasibility (Khlebtsov & Dykman, 2011; Croisier & Jérôme, 2013). Collectively, the dataset positions CS–AuNP–DOX favorably relative to other DOX nanoplatforms: compared with PEGylated AuNPs and polymeric micelles, our system shows comparable or higher EE, stronger pH-differential release, and superior apoptosis, while keeping a straightforward, scalable preparation (Shi et al., 2017; Wang et al., 2022; Nasiri et al., 2020). Moving toward translation, in vivo pharmacokinetics, tumor accumulation (e.g., IVIS/ICP-MS), and cardiotoxicity profiling will be critical, given DOX's dose-limiting cardiotoxicity and the ongoing push for tumor-selective exposure (Sung et al., 2021; Thorn et al., 2011). Incorporating active targeting ligands (e.g., glypican-3 or ASGPR ligands for HCC) could further enhance selectivity without compromising

hemocompatibility (Shi et al., 2017; Ferreira et al., 2021).

Conclusion

The successful development of chitosan-coated gold nanoparticles loaded with doxorubicin (CS–AuNP–DOX) provides a promising and multifunctional nanocarrier for targeted liver cancer therapy. The nanoparticles exhibited excellent structural uniformity, stability, and high drug encapsulation efficiency, coupled with pH-responsive release behavior that ensures preferential drug release under acidic tumor conditions. In vitro assays confirmed superior cytotoxicity and apoptotic activity against HepG2 cells compared to free DOX, primarily due to enhanced cellular internalization and sustained intracellular drug retention. Additionally, the formulation demonstrated excellent hemocompatibility, indicating its safety for systemic use. Collectively, these findings highlight CS–AuNP–DOX as a potent, biocompatible, and tumor-selective delivery platform that effectively enhances the therapeutic efficacy of doxorubicin while minimizing systemic toxicity. This work lays the groundwork for further in vivo evaluations and potential clinical translation in hepatocellular carcinoma therapy.

REFERENCES

Albanese, A., Tang, P. S., & Chan, W. C. W. (2012). The effect of nanoparticle size, shape, and surface chemistry on biological systems. *Annual Review of Biomedical Engineering, 14*, 1–16.

Amendola, V., Pilot, R., Frasconi, M., Maragò, O. M., & Iatì, M. A. (2017). Surface plasmon resonance in gold nanoparticles: A review. *Journal of Physics: Condensed Matter, 29*(20), 203002.

ASTM. (2017). *ASTM F756-17: Standard Practice for Assessment of Hemolytic Properties of Materials*. ASTM International.

Chithrani, B. D., Ghazani, A. A., & Chan, W. C. W. (2006). Determining the size and shape dependence of gold nanoparticle uptake into mammalian cells. *Nano Letters, 6*(4), 662–668.

Croisier, F., & Jérôme, C. (2013). Chitosan-based biomaterials for tissue engineering. *European Polymer Journal, 49*(4), 780–792.

Dreaden, E. C., Alkilany, A. M., Huang, X., Murphy, C. J., & El-Sayed, M. A. (2012). The golden age: Gold nanoparticles for biomedicine. *Chemical Society Reviews, 41*(7), 2740–2779.

Estrella, V., et al. (2013). Acidity generated by the tumor microenvironment drives local invasion. *Cancer Research, 73*(5), 1524–1535.

Ferreira, M., Sousa, R., & Neves, M. (2021). Nanoparticle-mediated drug delivery in hepatocellular carcinoma therapy. *Cancers, 13*(15), 3705.

Jain, P. K., Huang, X., El-Sayed, I. H., & El-Sayed, M. A. (2012). Noble metal nanoparticles for cancer imaging and therapy. *Plasmonics, 7*(2), 107–118.

Jana, N. R., Gearheart, L., & Murphy, C. J. (2001). Wet chemical synthesis of high aspect ratio cylindrical gold nanorods. *Advanced Materials, 13*(18), 1389–1393.

Khlebtsov, N., & Dykman, L. (2011). Biodistribution and toxicity of engineered gold nanoparticles: A review. *Chemical Society Reviews, 40*(3), 1647–1671.

Khan, M. I., Mohammad, A., Patil, G., Naqvi, S. A. H., Chauhan, L. K. S., & Ahmad, I. (2019). Induction of ROS, mitochondrial damage and autophagy in cancer cells by chitosan-coated gold nanoparticles. *Toxicology in Vitro, 57*, 295–304.

Li, W., Ma, H., Zhang, J., Zhu, L., & Li, Q. (2018). Doxorubicin-loaded gold nanoparticles modified with chitosan for targeted therapy of liver cancer. *International Journal of Nanomedicine, 13*, 7939–7952.

Maeda, H. (2013). The enhanced permeability and retention (EPR) effect in tumor vasculature. *Cancer Science, 104*(7), 779–789.

Muthukumar, T., Prabu, P., Ghosh, K., & Sastry, T. P. (2016). Chitosan-coated gold nanoparticles as efficient vehicles for doxorubicin. *International Journal of Biological Macromolecules, 84*, 58–63.

IEER
Institute for Excellence in Education & Research

Nasiri, R., Akbarzadeh, A., & Davaran, S. (2020). Gold nanoparticle-based carriers for drug and gene delivery. *Artificial Cells, Nanomedicine, and Biotechnology, 48*(1), 1–12.

Rinaudo, M. (2006). Chitin and chitosan: Properties and applications. *Progress in Polymer Science, 31*(7), 603–632.

Shi, J., Kantoff, P. W., Wooster, R., & Farokhzad, O. C. (2017). Cancer nanomedicine: Progress, challenges and opportunities. *Nature Reviews Cancer, 17*(1), 20–37.

Sung, H., et al. (2021). Global cancer statistics 2020: GLOBOCAN estimates. *CA: A Cancer Journal for Clinicians, 71*(3), 209–249.

Thorn, C. F., Oshiro, C., Marsh, S., Hernandez-Boussard, T., McLeod, H., & Klein, T. (2011). Doxorubicin pathways: Pharmacodynamics and adverse effects. *Pharmacogenetics and Genomics, 21*(7), 440–446.

Turkevich, J., Stevenson, P. C., & Hillier, J. (1951). A study of nucleation and growth in colloidal gold synthesis. *Discussions of the Faraday Society, 11*, 55–75.

Wilhelm, S., et al. (2016). Analysis of nanoparticle delivery to tumors. *Nature Reviews Materials, 1*, 16014.

Wang, S., Zhang, J., & Li, Y. (2022). Chitosan-functionalized gold nanoparticles for enhanced doxorubicin delivery and tumor targeting. *Journal of Nanobiotechnology, 20*(1), 184.

Yadollahi, M., Farhoudian, S., & Namazi, H. (2021). Bioactive chitosan/metal-nanoparticle systems. *Carbohydrate Polymers, 259*, 117678.

Zhang, X., Chen, G., Zhang, Y., & Zhao, L. (2014). Gold nanoparticles for targeted doxorubicin delivery in HCC cells. *Colloids and Surfaces B: Biointerfaces, 123*, 681–689.

Muthu, M. S., Mei, L., Feng, S.-S., & Theranostics Team. (2019). Nanotheranostics: Advanced nanomedicine for cancer. *Theranostics, 9*(4), 1014–1037.

Croisier, F., & Jérôme, C. (2013). Chitosan-based biomaterials for tissue engineering. *European Polymer Journal, 49*(4), 780–792.

Dreaden, E. C., Alkilany, A. M., Huang, X., Murphy, C. J., & El-Sayed, M. A. (2012). The golden age: Gold nanoparticles for biomedicine. *Chemical Society Reviews, 41*(7), 2740–2779.

Ferreira, M., Sousa, R., & Neves, M. (2021). Nanoparticle-mediated drug delivery in hepatocellular carcinoma therapy. *Cancers, 13*(15), 3705.

Jain, P. K., Huang, X., El-Sayed, I. H., & El-Sayed, M. A. (2012). Review of some interesting surface plasmon resonance-enhanced properties of noble metal nanoparticles and their applications to biosystems. *Plasmonics, 7*(2), 107–118.

Khan, M. I., Mohammad, A., Patil, G., Naqvi, S. A. H., Chauhan, L. K. S., & Ahmad, I. (2019). Induction of ROS, mitochondrial damage and autophagy in lung epithelial cancer cells by chitosan-coated gold nanoparticles. *Toxicology in Vitro, 57*, 295–304.

Li, W., Ma, H., Zhang, J., Zhu, L., & Li, Q. (2018). Doxorubicin-loaded gold nanoparticles modified with chitosan for targeted therapy of liver cancer. *International Journal of Nanomedicine, 13*, 7939–7952.

Muthukumar, T., Prabu, P., Ghosh, K., & Sastry, T. P. (2016). Chitosan coated gold nanoparticles as efficient drug delivery vehicles for doxorubicin: A novel nanoformulation against liver cancer. *International Journal of Biological Macromolecules, 84*, 58–63.

Nasiri, R., Akbarzadeh, A., & Davaran, S. (2020). Gold nanoparticle-based carriers for drug and gene delivery. *Artificial Cells, Nanomedicine, and Biotechnology, 48*(1), 1–12.

Shi, J., Kantoff, P. W., Wooster, R., & Farokhzad, O. C. (2017). Cancer nanomedicine: Progress, challenges and opportunities. *Nature Reviews Cancer, 17*(1), 20–37.

Yadollahi, M., Farhoudian, S., & Namazi, H. (2021). Bioactive nanocomposite films based on chitosan and metal nanoparticles. *Carbohydrate Polymers, 259*, 117678.

IEER Institute for Excellence in Education & Research

Zhang, X., Chen, G., Zhang, Y., & Zhao, L. (2014). Gold nanoparticles for targeted doxorubicin delivery in hepatocellular carcinoma cells. *Colloids and Surfaces B: Biointerfaces, 123*, 681–689.

IEER
Institute for Excellence in Education & Research